

A Test Case for GIC Harmonics Analysis

A. OVALLE, R. DUGAN, R. ARRITT
Electric Power Research Institute (EPRI)
USA

SUMMARY

Geomagnetically-Induced Currents (GIC) are very low-frequency currents due to the electromagnetic field induced in the earth caused by solar Geomagnetic Disturbances (GMD) such as coronal mass ejections.

For analysis purposes, the frequencies are so low that the currents may be represented as direct currents (dc) on the bulk power system. The induced currents flow through the transmission system and complete the circuit through the neutral paths in grounded-wye transformers. This quasi-dc current causes part-cycle saturation of the magnetic circuit of the transformer, yielding highly-distorted exciting currents containing both even and odd harmonics. This results in high harmonic currents in transformers, generators, and capacitor banks in the bulk power system that can damage these power delivery elements.

The capability to estimate the GIC has been incorporated into common power flow tools used in transmission system planning. However, this has not been combined with frequency-domain harmonics analysis tools. The main alternative has been to use electromagnetic transients program with lengthy run times and complicated model setups that are unfamiliar to many planning engineers.

EPRI has been researching this problem since before 2014 and has developed system analysis tool requirements needed to conduct GIC related harmonic analysis [1]. This has resulted in the development of the GICcharm tool that takes GIC data from a variety of sources and computes estimates of the harmonic distortion throughout the power transmission system. The current waveforms from saturated transformers are computed in the time domain using a Python module and are used to populate the harmonic flow model of the transmission network. The network is modelled in the frequency domain using EPRI's open-source OpenDSS tool. OpenDSS is a general nodal admittance multi-phase circuit solver that uses methods derived from harmonics solvers. GICcharm iterates between the time-domain and frequency-domain solvers to achieve the final result.

Because GICcharm is the first tool of its kind, this paper presents a small benchmark case to provide other researchers with a reference for other similar tools they might develop.

KEYWORDS

Geomagnetic Disturbances, GMD, Geomagnetically-Induced Currents, GIC, Magnetizing Current Harmonics, Harmonic System Analysis

DESCRIPTION OF GICcharm

The overall GIC harmonics approach implemented in the EPRI GICcharm program is illustrated in the flow chart in Figure 1. The software is based on the EPRI OpenDSS program with Python-language auxiliary programs for time-domain solution and for importing data from other sources. The main network model is first constructed in the OpenDSS program. The GIC values are either computed using the OpenDSS model or imported from other computer tools in the industry capable of computing the GIC values given the GMD electric field values. A basic power flow calculation at fundamental frequency is then made. This may also be imported from another computer program's power flow results. This initializes the process.

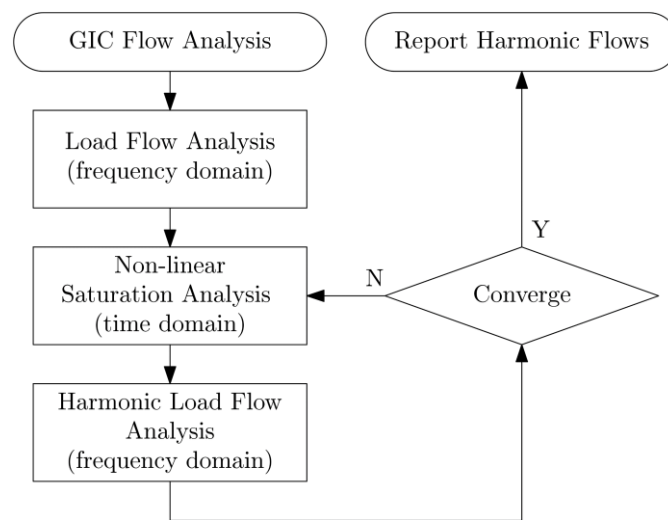


Figure 1. GICcharm Software Overall Algorithm

Non-Linear Saturation Analysis

After initializing the algorithm with a Load Flow analysis, the next step is to run the Non-linear Saturation Analysis routine mentioned in Figure 1. This routine is used to obtain the spectra of excitation currents drawn by transformers exposed to GIC. This routine solves magnetic circuits and finds DC flux linkages over a power-cycle, to characterize the response of different transformer core topologies, i.e., 3-leg core, 5-leg core, shell-form and single-phase cores. These core topologies are represented by the magnetic circuits shown in Figure 2 [3][4]. GICcharm defines the flux linkage sources in these models in discrete time steps by reconstructing time-domain voltages across transformer windings from their spectra. These spectra are given by the initial power flow (only fundamental frequency at the first GICcharm iteration) or by the harmonics solution (at subsequent GICcharm iterations). Numerically integrating these voltage waveforms over time results in the flux linkages in discrete time steps.

As shown in Figure 2, a core topology is represented by a set of flux linkage sources, linear reluctances, and non-linear reluctances forming a magnetic circuit. In an ideal scenario with only linear reluctances, the magnetic circuit could be described by a linear expression in nodal “permeance” form (analog to the familiar nodal admittance form). However, since the flux paths in a core topology saturate, the nodal admittance representation of the magnetic circuit needs to be adapted to represent the non-linear saturation behavior. GICcharm models saturable reluctances as piece-wise linear reluctances, and

iteratively adapt the nodal “permeance” form expression for each time step and flux linkage source. The routine iteratively solves for DC-flux linkages and excitation currents, given GIC currents and flux linkage values over time.

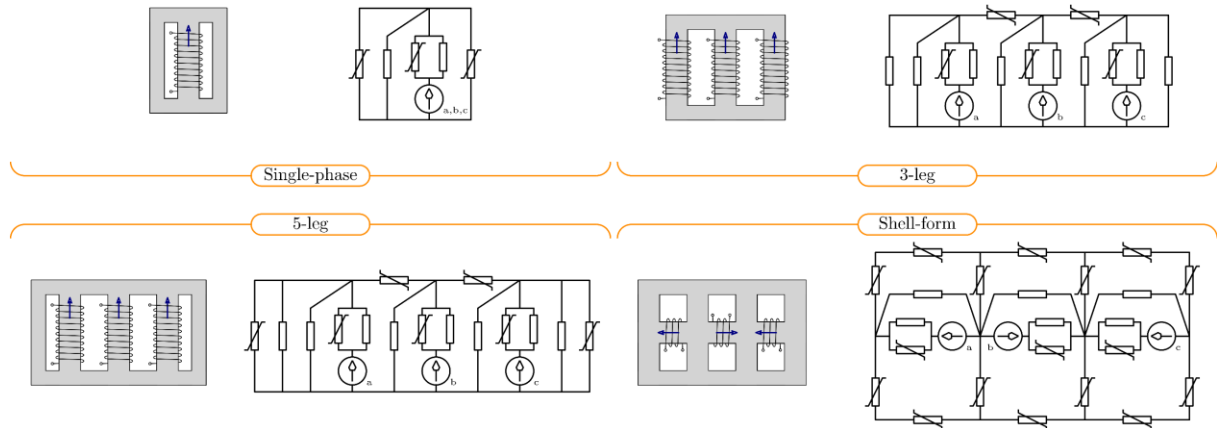


Figure 2. Core-Topologies and Magnetic Circuit Models in GICcharm

Figure 3 shows the excitation current characteristic waveforms per phase of transformers with 5-leg and shell-form core topologies exposed to of 0.02 p.u. GIC. These are obtained with the transformer level modelling capability of GICcharm with only fundamental frequency voltage. The interactions of injected harmonic currents with impedances in the system may result in voltages with nonzero harmonic content, which in turn may result in excitation current responses different than that of Figure 3.

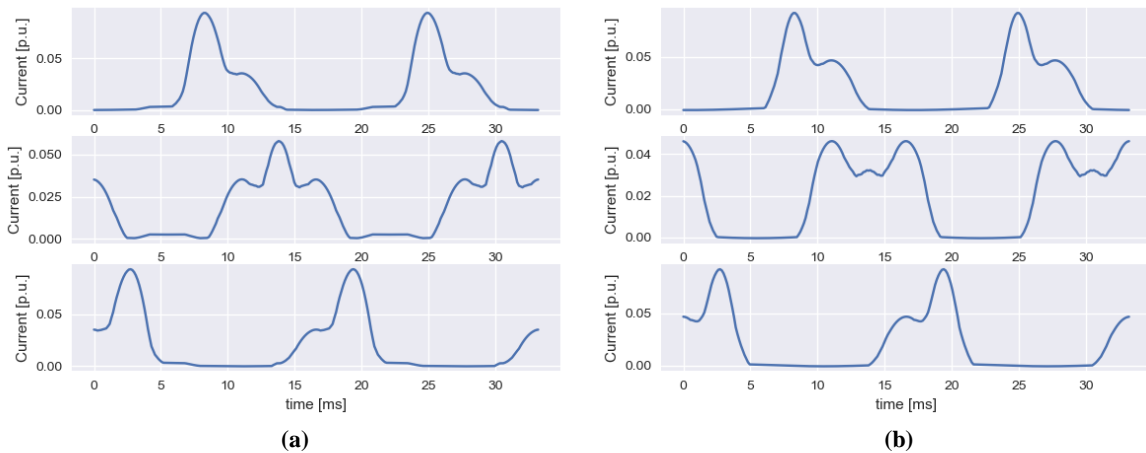


Figure 3. Excitation current waveforms (phases A to C from top to bottom) for transformers exposed to 0.02p.u. GIC. (a) 5-leg core; (b) Shell-form

In the OpenDSS model, the computed excitation current spectra per phase are then attached to a Load object in each phase connected to a fictitious extra wye-connected winding in the transformer object. The fundamental frequency active and reactive power properties of these load objects are given by the fundamental components of the excitation currents and the voltages used to compute the discrete time flux linkage sources. This is the approach used by GICcharm to represent the magnetizing branch of each transformer in the OpenDSS model. More details on the load model of OpenDSS are described in the following section of the paper.

The non-linear saturation analysis routine computes the excitation current spectra of all the transformers across the system.

Once the magnetizing branch parameters of each transformer across the system are defined, the next step is to run a harmonic power flow analysis as shown in Figure 1. The basic equation solved by OpenDSS is the familiar nodal admittance formulation,

$$\mathbf{i}_{inj} = \mathbf{Y}_{SYS} \mathbf{v}, \quad (1)$$

where \mathbf{v} is the vector of node voltages, \mathbf{i}_{inj} is the vector of injection currents at each node from non-linear elements, harmonic sources, etc., and \mathbf{Y}_{SYS} is the Nodal admittance matrix representing linear element admittances.

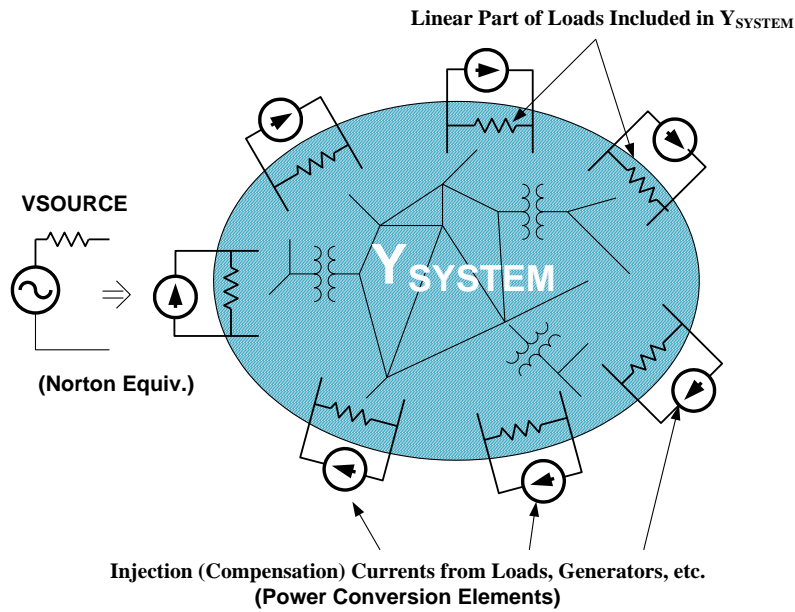


Figure 4. OpenDSS Circuit Model

Nonlinear elements such as loads, generators, and the transformer magnetizing impedances are modeled as Norton equivalents as shown in Figure 4. The linear admittances of the Norton equivalents are included in the \mathbf{Y}_{SYS} matrix while the current sources make up the components of the \mathbf{i}_{inj} vector.

All Load-class elements in OpenDSS have a harmonic spectrum associated with them as shown in Figure 5. As mentioned previously, this Load model is used to represent the transformer magnetizing currents in the GICHarm analysis procedure. In the Harmonic Load-Flow analysis the magnetizing element of each transformer in the model is represented by an OpenDSS load element with its fundamental frequency active and reactive power values set to the values determined from the non-linear saturation analysis step.

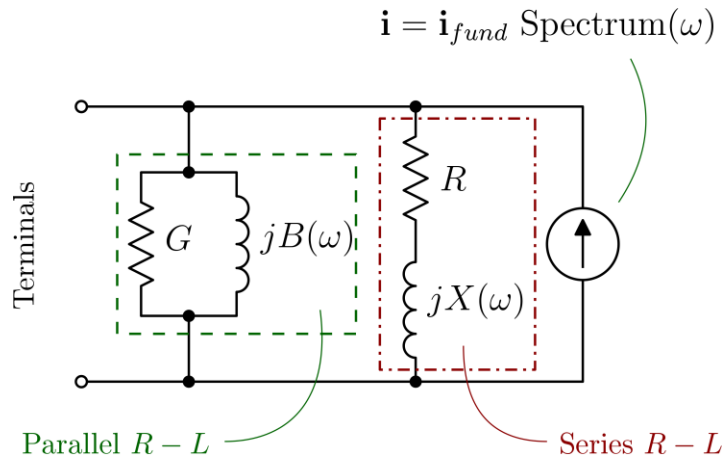


Figure 5. Detail on Load Model for Harmonics Solution [2]

For power flow analysis in OpenDSS, the injection currents typically represent the nonlinear voltage dependence of the loads and (1) is solved iteratively at fundamental frequency. For harmonics power flow analysis, the injection currents represent the harmonic currents from the various nodes with distorted currents. After a fundamental frequency solution, OpenDSS executes a linear, non-iterative solution at each frequency present in the various harmonic sources in the problem.

After the harmonic load flow analysis is complete, the spectra of voltages across transformer windings is used again to reconstruct the time domain voltage waveforms and the flux linkage waveforms as well. This is then used to run the non-linear saturation analysis routine once again. This process is repeated until a suitable convergence for the harmonic current components is reached.

SIMPLE TEST CASE CIRCUIT

The circuit shown in Figure 6 is a simple 3-bus system proposed for researchers as a reference for similar tools they might develop. The system is composed of three 500 kV buses, three transmission lines, two two-winding generator step-up transformers, one three-winding transformer with a delta tertiary, two generators, one load, and two capacitors.

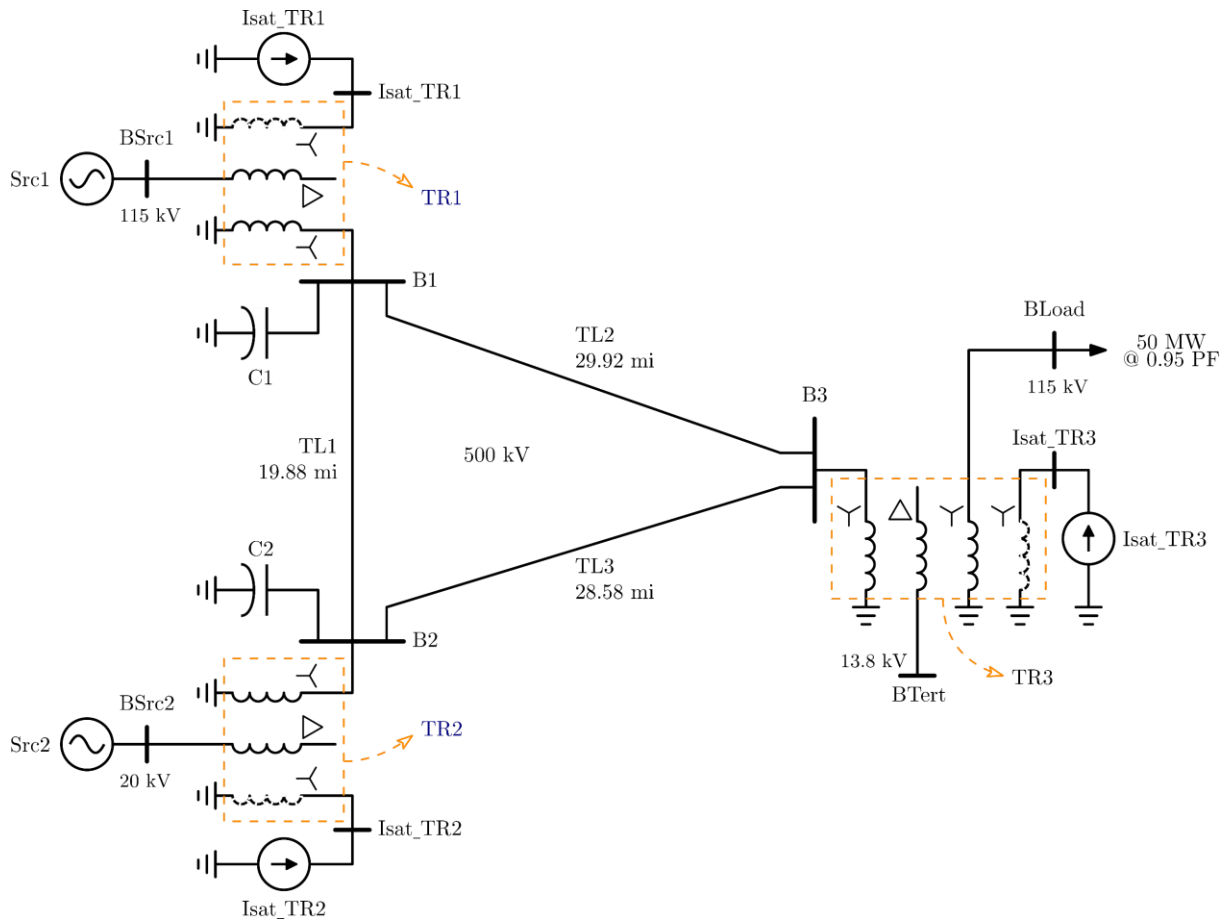


Figure 6. Simple 3-Bus Test Case

As previously described, the magnetizing branch of each transformer is represented by a fictitious extra grounded-wye winding with a current source attached. The current source is modeled using an OpenDSS Load element that ultimately is represented as a Norton equivalent current source. The transformer parameters are listed in Table 1.

The coordinates of the main buses B1, B2, B3 are listed in Table 2, as well as other buses sharing the same location. The system is randomly located in the northeastern region of the state of Georgia in the United States. It is important to mention that the location of these buses is fictitious and doesn't reveal any critical infrastructure information.

Two capacitor banks are located at Buses B1 and B2 respectively. Their parameters are described in Table 3.

Table 1 Transformer parameter names and values

Parameters	Transformer Name		
	TR1	TR2	TR3
Number of windings (+1 for magnetizing branch)	2 (+1)	2 (+1)	3 (+1)
Reactance winding 1 to 2	12%	12%	12%
Reactance winding 1 to 3	7%	7%	35%
Reactance winding 1 to 4	-	-	9.5%
Reactance winding 2 to 3	7%	7%	30%

Reactance winding 2 to 4	-	-	4.5%
Reactance winding 3 to 4	-	-	27.5%
Resistance winding 1	0.5%	0.5%	0.5%
Resistance winding 2	0.5%	0.5%	0.5%
Resistance winding 3	0.1%	0.1%	0.5%
Resistance winding 4			0.1%
MVA ratings of all windings	1000 MVA	500 MVA	100 MVA
Winding voltage bases	115 kV	500 kV	500 kV
	500 kV	20 kV	13.8 kV
	24.9 kV	24.9 kV	115 kV
Winding connections	Delta	Wye	Wye
	Wye	Delta	Delta
	Wye	Wye	Wye
Core	3 single-phase	5-leg	3-leg

Table 2 Bus parameters and values

Parameters	Main Bus Name		
	B1	B2	B3
Latitude	33.813358°	33.523973°	33.642800°
Longitude	-82.797760°	-82.797760°	-82.319137°
Buses with same coordinates	B1	B2	B3
	B1	B2	B3
	B1	B2	B3
	B1	B2	B3

Table 3 Capacitor parameters and values

Parameters	Capacitor Name	
	C1	C2
Bus	B1	B2
Total reactive power	10 Mvar	10 Mvar

As described previously, three lines connect the main three buses and their parameters are listed in Table 4.

The following section tests the proposed system under different GMD event characteristics. An analysis of the response of the system is provided as well.

Table 4 Line parameters and values

Parameters	Line Name		
	TL1	TL2	TL3
Length	19.88 mi	29.92 mi	28.58 mi
Resistance phase 1	0.087405303 Ω /mile		
Resistance phase 2	0.088371212 Ω /mile		
Resistance phase 3	0.086666667 Ω /mile		
Resistance phase 1 to 2	0.029924242 Ω /mile		
Resistance phase 1 to 3	0.029071970 Ω /mile		

Resistance phase 2 to 3	0.029545455 Ω /mile		
Reactance phase 1	0.201723485 Ω /mile @60 Hz		
Reactance phase 2	0.198522727 Ω /mile @60 Hz		
Reactance phase 3	0.204166667 Ω /mile @60 Hz		
Reactance phase 1 to 2	0.198522727 Ω /mile @60 Hz		
Reactance phase 1 to 3	0.072897727 Ω /mile @60 Hz		
Reactance phase 2 to 3	0.095018939 Ω /mile @60 Hz		
Nodal Capacitance phase 1	2.711347560 nF/mile		
Nodal Capacitance phase 2	3.004631862 nF/mile		
Nodal Capacitance phase 3	2.851710072 nF/mile		
Nodal Capacitance phase 1 to 2	0.585011253 nF/mile		
Nodal Capacitance phase 1 to 3	-0.350755566 nF/mile		
Nodal Capacitance phase 2 to 3	-0.920293787 nF/mile		
Bus 1	B1	B1	B2
Bus 2	B2	B3	B3

TEST CASE RESULTS

An initial power flow shows voltage magnitudes at buses B1, B3 at 1.044 p.u. and 1.045 p.u. at bus B2. For this test, let us consider a GMD event with 2 V/km electric field magnitude pointing to the northeast at 45° inclination (eastward and northward field components equally valued to $\sqrt{2}$ V/km). Figure 7(a) shows a geographic view of the circuit with labels showing the location of buses B1, B2, and GIC currents beside each line. For line TL1, the figure shows the direction of GIC, flowing from bus B1 to bus B2. Figure 7(b) shows the geographic view of the circuit including the GIC flow direction and value for each line. As it may be expected the disposition of line TL2 with respect to the direction of the electric field makes it less susceptible to current induction, as opposed to TL1 and TL3.

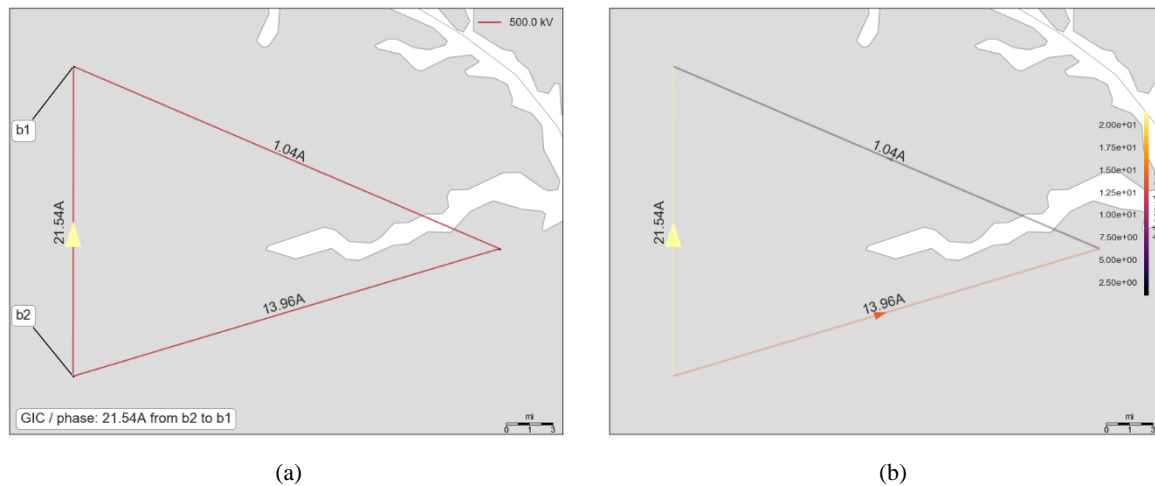


Figure 7 (a) Circuit geographical view; (b) GIC flow directions and values

The GIC flows into each transformer per phase are 22.576 A, -35.5 A and 12.924 A for TR1, TR2 and TR3 respectively. These values can be verified with the currents flowing through each line into and out of each bus in Figure 7(b). Figure 8 shows the magnetizing current waveforms per phase of transformer TR2 (5-leg core) for this scenario after the 1st and 10th iterations under the considered GMD event. The GIC base is assumed to be the peak rated current (1633 A for TR2). Although changes can be noticed, especially in phase B, a look at the spectrum per phase could be more useful.

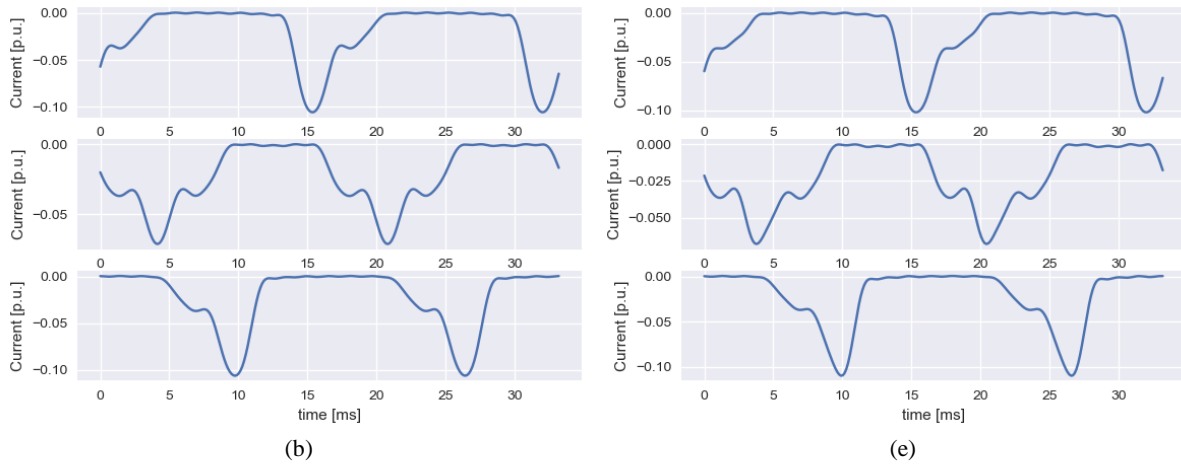


Figure 8 Excitation current waveforms per phase (transformer TR2) after the 1st iteration (left side) and the 10th iteration (right side) of the harmonics loop. From top to bottom, waveforms for phases A, B, C.

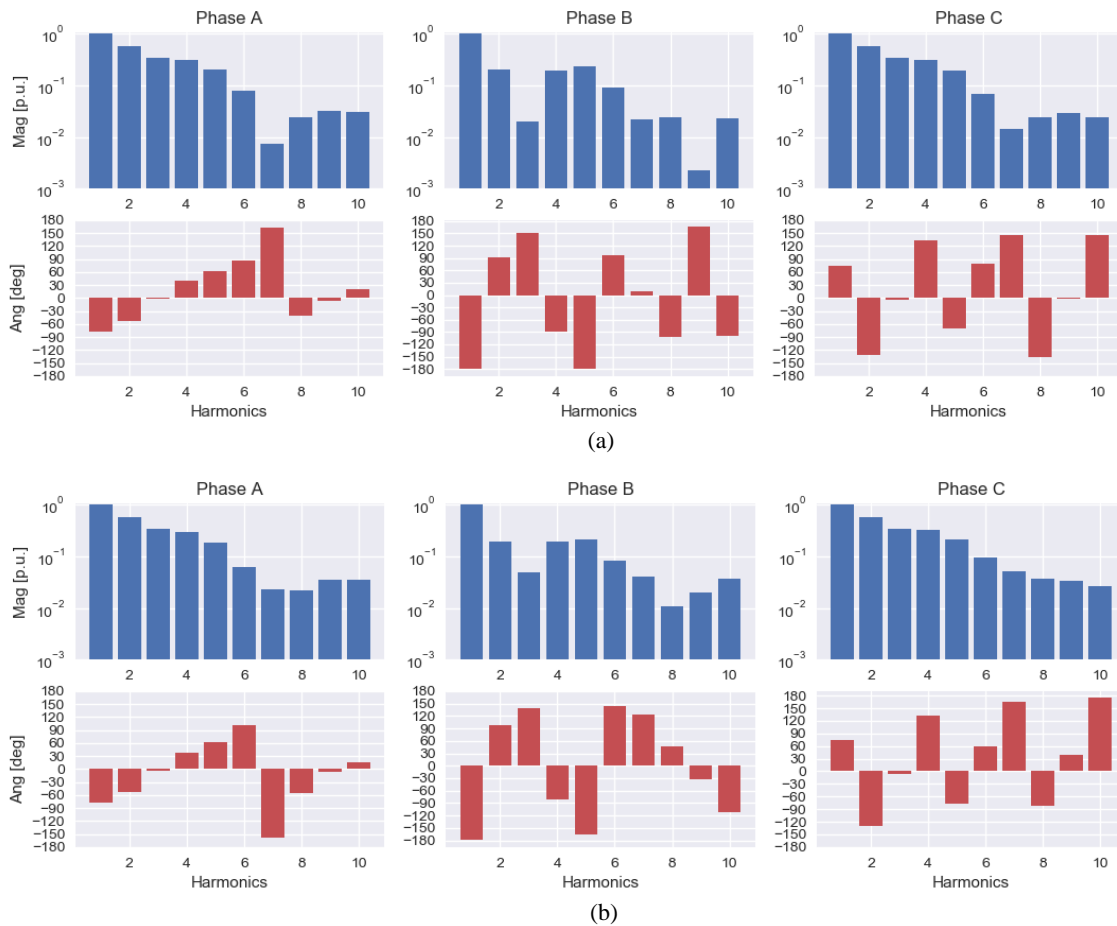


Figure 9 Excitation current spectrum per phase for transformer TR2 after the 1st iteration (a) and the 10th iteration (b)

Figure 9 shows the spectra corresponding to these waveforms. A close look at these spectra reveals an accentuation of the 7th harmonic across the three phases, as well as an increase in the 3rd and 9th harmonics on phase B. However, the differences are rather small because the source at bus BSrc1 is relatively stiff, not allowing high voltage distortions at the 500-kV level.

After the 10th iteration, the reactive power losses per phase for each transformer during this GMD event are listed in Table 5. Since T3 has a 3-leg core topology, its losses in TR3 are relatively low compared to those of TR1 and TR2.

Table 5 GIC and reactive power losses per phase during the GMD event of the example

Parameter	Transformer Name		
	TR1	TR2	TR3
GIC/phase	22.576 A	-35.5 A	12.924 A
Reactive power loss – Phase A	9.29 Mvar	11.74 Mvar	0.3 Mvar
Reactive power loss – Phase B	9.32 Mvar	9.67 Mvar	0.3 Mvar
Reactive power loss – Phase C	9.14 Mvar	11.99 Mvar	0.3 Mvar

These reactive power losses impact the voltage profile across the network. The evolution of the voltage magnitude at the fundamental frequency at bus B2 is shown in Figure 10. For this GMD event, fundamental voltage magnitudes settle around 1.0385 p.u. for buses B1 and B2, and 1.037 p.u. for bus B3.

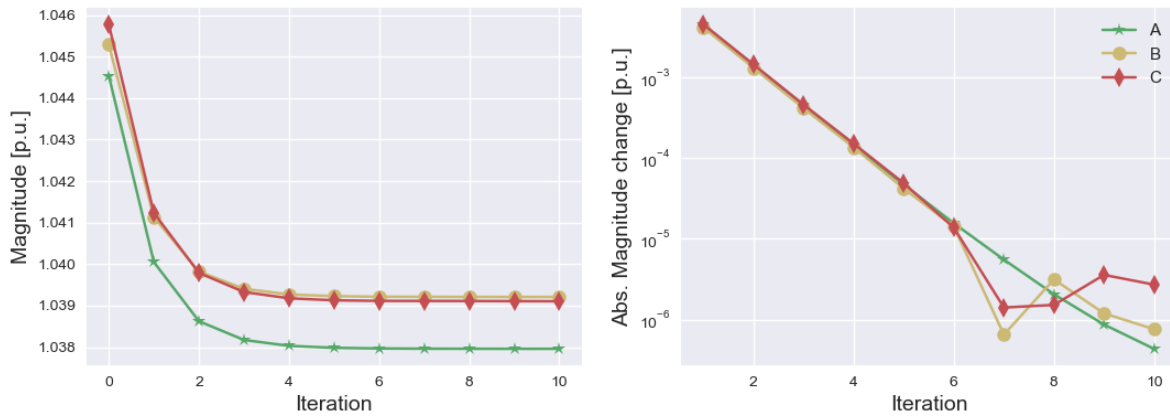


Figure 10 (Left) Evolution of the fundamental voltage magnitude at bus B2. (Right) Absolute magnitude change between iterations. Iteration 0 corresponds to the initial magnitude before the GMD event.

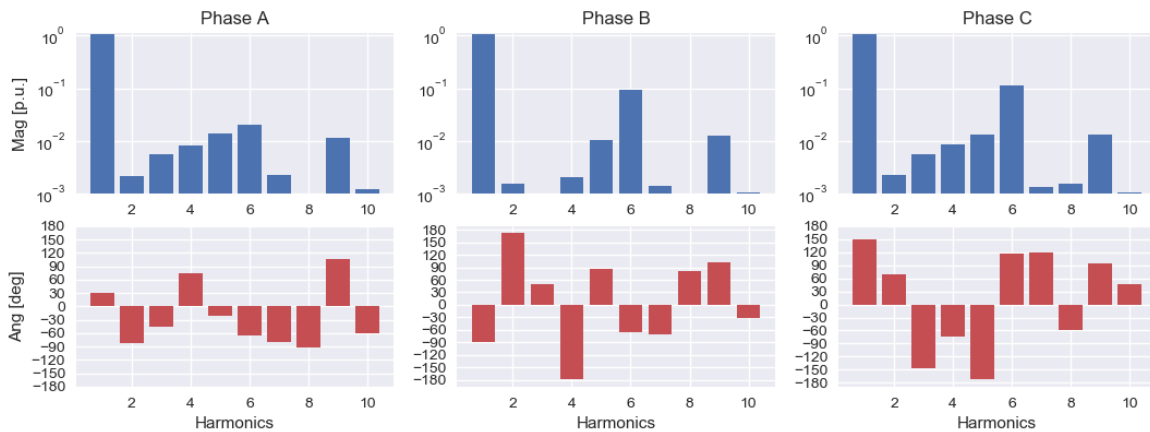


Figure 11 Spectrum per phase of the voltage at bus B2 after the 10th iteration

The voltage spectrum at bus B2 is shown in Figure 11. The 6th harmonic has the highest magnitude, especially in phases B and C. This is mostly due to the unbalanced harmonic injection caused by saturation characteristic of 5-leg cores. The 9th harmonic and harmonics below the 6th are also present but their magnitudes are smaller than the 6th. To understand the effect of the harmonics injected to the system during a GMD event, a frequency scan at a given bus may reveal relevant information. For this test case, frequency scans at the three main buses reveal a frequency resonance around the 9th harmonic order. Figure 12 shows the results of this frequency scan at bus B1. This frequency scan is obtained by injecting 1.0 A at each frequency between 60 Hz and 600 Hz (10th harmonic order). The scan also reveals

resonances at frequencies around the 6th harmonic order. The resonance around the 9th harmonic is the cause of its presence in the voltage spectrum. However, it is not as high as that of the 6th and lower orders because the amount of 9th harmonic of current injected to the system is comparatively small.

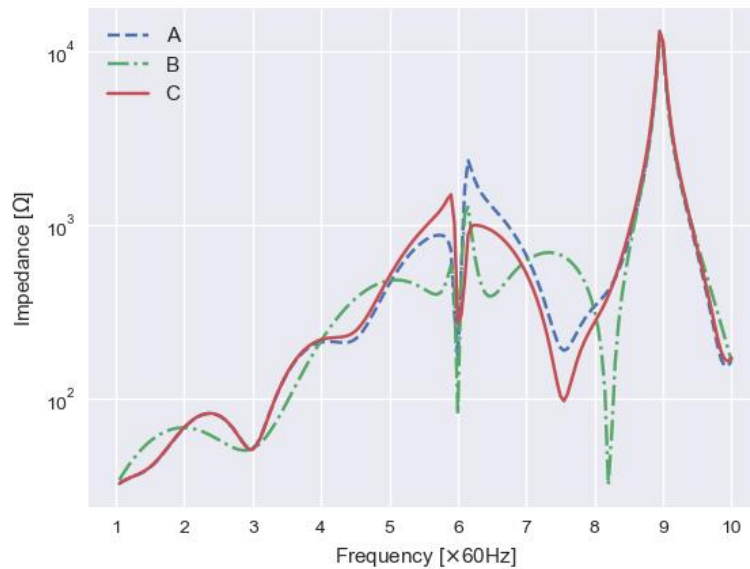


Figure 12 Frequency sweep of 1A current injected at bus B1

Table 6 THD values at transmission level buses

Parameter	Bus Name		
	B1	B2	B3
Voltage THD - Phase A	2.76%	2.83%	2.81%
Voltage THD – Phase B	8.90%	9.09%	9.03%
Voltage THD – Phase C	10.70%	10.95%	10.85%

A summary of the Voltage THD values is provided in Table 6. The higher THD are observed in phases B and C, this reflects on the result shown in the voltage spectrum at bus B2.

CONCLUSIONS

The study of harmonic impact of saturated transformers due to GIC is a relatively new field for which few computer tools exist. This paper provides a relatively simple, yet challenging, test case for students, researchers, and developers to learn the field and advance it so that practical networks may be studied.

BIBLIOGRAPHY

- [1] Analysis of Geomagnetic Disturbance (GMD) Related Harmonics. EPRI, Palo Alto, CA: 2014. 3002002985.
- [2] D. Montenegro, R. Dugan, Gustavo Ramos, “Harmonics Analysis using Sequential-Time Simulation for Addressing Smart Grid Challenges, CIRED 2015, Lyon, Paper 0946.
- [3] Electromagnetic transient-type transformer models for Geomagnetically-Induced Current (GIC) studies. EPRI, Palo Alto, CA: 2013. 3002000832.
- [4] R. A. Walling and A. N. Khan, "Characteristics of transformer exciting-current during geomagnetic disturbances," in IEEE Transactions on Power Delivery, vol. 6, no. 4, pp. 1707-1714, Oct. 1991. doi: 10.1109/61.97710